Direct Mass Spectrometric Determination of the Stoichiometry and Binding Affinity of the Complexes between Nucleocapsid Protein and RNA Stem−Loop Hairpins of the HIV-1 Ψ-Recognition Element†

Nathan Hagan and Daniele Fabris*

Department of Chemistry and Biochemistry, University of Maryland, Baltimore County, Baltimore, Maryland 21250

Received May 26, 2003; Revised Manuscript Received July 21, 2003

ABSTRACT: The formation of noncovalent complexes between the HIV-1 nucleocapsid protein p7 (NC) and RNA hairpins SL2−SL4 of the Ψ-recognition element was investigated by direct infusion electrospray ionization-Fourier transform mass spectrometry (ESI-FTMS). The high resolution afforded by this method provided the unambiguous characterization of the stoichiometry and composition of complexes formed by multiple equilibria in solution. For each hairpin, the formation of a 1:1 complex was found to be the primary binding mode in solutions of intermediate salt content (150 mM ammonium acetate). Binding of multiple units of NC was observed with lower affinity and a maximum stoichiometry matching the limit calculated from the number of nucleotides in the construct and the size of the footprint of NC onto single-stranded nucleic acids, thus implying the defolding of the hairpin three-dimensional (3D) structure. Dissociation constants of 62 ± 22 nM, 178 ± 64 nM, and 1.3 ± 0.5 μM were determined for SL2, SL3-2, and SL4, respectively, which are similar to values obtained by spectroscopic and calorimetric methods with the additional confidence offered by a direct, rather than inferred, knowledge of the binding stoichiometry. Competitive binding experiments carried out in solutions of intermediate ionic strength, which has the effect of weakening the electrostatic interactions in solution, provided a direct way of evaluating the stabilizing contributions of H-bonding and hydrophobic interactions that are more sensitive to the sequence and structural context of the different hairpins. The relative scale of binding affinity obtained in this environment reflects the combination of contributions provided by the different structures of both the tetraloop and the double-stranded stem. The importance of the stem 3D structure in modulating the binding activity was tested by a competitive binding experiment that included the SL3-2 RNA construct, a DNA analogue of SL3 ($SL3_{DNA}$), and a DNA analogue in which all four loop bases were replaced with abasic nucleotides ($SL3_{abasic}$). NC was found to bind the A-type double-stranded stem of SL3-2 RNA at least 30 times more tightly than the B-type helical structure of $SL3_{DNA}$. Eliminating the stabilization provided by the interactions with the tetraloop bases made the binding of $SL3_{abasic}$ ∼50 times weaker than that of $SL3_{DNA}$.

In mature retroviral virions, genetic information is encoded by two homologous strands of genomic RNA packaged in a dimeric form (*1*). During the assembly of human immunodeficiency virus type 1 (HIV-1),[1] the crucial processes of strand recognition, dimerization, and packaging are mediated by the interaction of the nucleocapsid protein p7 (NC) (*2*−*4*) with a highly conserved stretch of genomic RNA located near the 5′-long terminal repeat, termed the packaging signal or Ψ-RNA (*5*−*7*).

NC corresponds to a 55-residue domain of the *Gag*/*Gag-Pol* polyprotein and includes two zinc-finger motifs of the retroviral type (CCHC) (*8*, *9*) (Figure 1), which are members of a large class of structural domains encountered in nucleic acid binding proteins (*10*). Either as a part of the larger *Gag* or as a proteolytic product formed during viral maturation (*11*), NC affords a broad spectrum of nucleic acid binding activity *in vivo* and *in vitro*, which includes RNA, single-stranded DNA, and double-stranded DNA (*12*−*17*). A detailed examination of the multifaceted functions performed by NC during the viral life cycle has led to the proposal that the protein acts as a nucleic acid chaperone by promoting conformational changes and by facilitating intermolecular interactions between nucleic acids (reviewed in refs *18* and *19*). Consistent with this suggestion, it was observed that binding is largely affected by the structural context of the nucleic acids (e.g., presence of elements of secondary structure) rather than by the presence of any particular nucleotide sequence or base composition (*17*).

Considerable efforts have been directed to understanding the structural determinants of the interaction between NC and Ψ-RNA with the ultimate goal of enabling the development of inhibitors aimed at disrupting the proper assembly

† This work was supported by the National Institutes of Health (Grant R01-GM643208).

* To whom correspondence should be addressed. Telephone: (410) 455-3053. Fax: (410) 455-2608. E-mail: fabris@umbc.edu.

[1] Abbreviations: HIV-1, human immunodeficiency virus type 1; NC, nucleocapsid protein; SL, stem−loop; ESI, electrospray ionization; MS, mass spectrometry; FTMS, Fourier transform mass spectrometry; ITC, isothermal titration calorimetry; NMR, nuclear magnetic resonance; EDTA, ethylenediaminetetraacetic acid; K_d, equilibrium dissociation constant; ΔV_{TS}, voltage potential difference between the metal tubing and the first skimmer in the electrospray source; *m*/*z*, mass-to-charge ratio.

10.1021/bi0348922 CCC: $25.00
Published on Web 08/16/2003

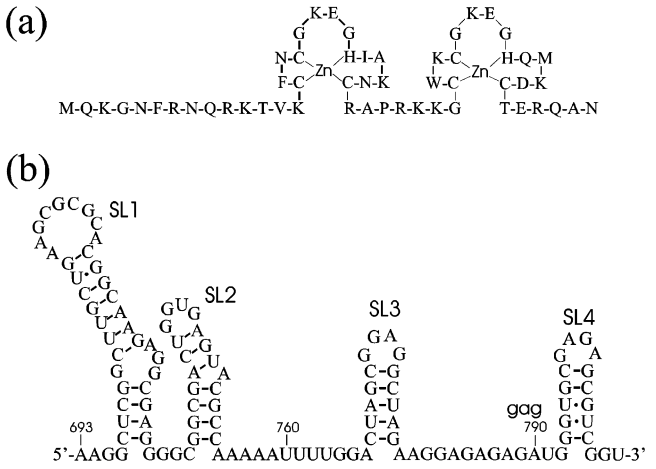

FIGURE 1: (a) Amino acid sequence of HIV-1 nucleocapsid protein. (b) Base sequence and secondary structure of HIV-1 Ψ-RNA, showing stem−loop hairpins 1−4 (SL1−SL4, respectively) and the *Gag* gene product transcription start site. The numbering starts from the 5′ end of the genome.

of viral particles. In the absence of a complete high-resolution structure for the ∼120 nucleotides forming the packaging signal, a combination of methods has led to a consensus map, which shows Ψ-RNA folded into relatively stable elements of secondary structure identified as stem−loop hairpins 1−4 (SL1−SL4, respectively, Figure 1) (*20*−*24*). While the role of each hairpin in the process of viral assembly has been probed through biological assays (*21*, *25*−*30*), the determinants of the interactions between NC and the different structures of Ψ-RNA have been extensively investigated by a variety of methods *in vitro*, including North-western blotting (*31*, *32*), filter binding assay (*20*, *33*−*35*), gel electrophoresis mobility shift (*14*, *31*, *36*−*38*), fluorescence and phosphorescence spectroscopy (*17*, *39*−*43*), nuclear magnetic resonance (*44*−*46*), and isothermal calorimetry (*45*, *46*).

An accurate determination of the stoichiometry and affinity of binding between NC and the hairpins would provide very valuable information about the possible sequence of events unfolding during genome recognition, dimerization, and packaging. Unfortunately, the picture emerging from the analysis of binding data provided by the different sources shows little consensus, which may be explained by the widely heterogeneous experimental conditions and by the significant effects of concentration and ionic strength on the binding process. For example, independent studies based on fluorescence quenching titrations resulted in either a 1:2 (*41*) or 1:1 (*42*) RNA to protein stoichiometry for the SL3·NC complex, despite the fact that these experiments employed similar RNA constructs and salt content. In an analogous situation, gel mobility experiments carried out independently under comparable conditions provided either a 2:1 (8:4) (*38*) or 1:1 RNA to protein ratio (1:2 was also observed at higher NC concentrations) (*46*) for the same SL3·NC complex. Table 1 provides a summary of the data concerning stoichiometry and binding affinity reported thus far for the complexes of NC with SL2−SL4 hairpins from HIV-1 Ψ-RNA.

In this report, the interactions between NC and these RNA hairpins are investigated *in vitro* by direct infusion electrospray ionization (ESI) (*47*, *48*) and Fourier transform mass spectrometry (FTMS) (*49*, *50*). ESI constitutes the method of choice for the investigation of multicomponent macromolecular complexes by mass spectrometry (*51*−*56*), because of the inherently low energy involved in the desolvation process and the use of compatible buffers, which help to stave off denaturation without deteriorating the analytical response. Careful selection of experimental conditions has enabled the observation of protein−nucleic acid complexes involving single-stranded oligodeoxynucleotides (*57*), double-stranded oligodeoxynucleotides (*58*−*63*), and RNA (*64*−*67*), providing very valuable information about binding stoichiometry and ligand identity. In some cases, an excellent correlation between the concentrations of the species in equilibrium and their signal intensities has enabled the determination of solution phase dissociation constants (K_d) for the complexes of proteins with mononucleotides (*68*) and both single- and double-stranded oligodeoxynucleotides (*57*, *62*, *69*). The dissociation constants for the binding of small ligands to RNA were determined in a similar way by electrospray ionization (*70*, *71*). The different MS-based methods employed for the determination of binding constants have been recently reviewed by Daniel *et al*. (*72*).

The combination of ESI with FTMS offers an excellent opportunity to obtain a direct and unambiguous characterization of the noncovalent complexes formed by interaction of NC with the different RNA hairpins under a wide range of binding conditions. Alternative spectroscopic and calorimetric methods can provide only an indirect determination of the stoichiometry of bound complexes, which is generally inferred from curve fitting procedures, while filter binding and electrophoretic methods rely on the separation of species in solution, which may affect the position of the binding equilibrium. On the contrary, the intrinsically high resolution afforded by FTMS has the potential to resolve any complex mixture of analytes, which may originate from multiple binding equilibria in solution. The high level of accuracy provided by this mass analyzer enables a direct determination

Table 1: Summary of Recent Studies Involving HIV-1 Ψ-PNA Hairpin·NC Complexes

RNA hairpin	K_d of the complex with NC	stoichiometry (RNA:protein)	method	salt content[a] (mM)	ref
SL2	∼400 nM	1:1	filter binding[b]	50	*20*
	110 ± 50 nM	1:1	ITC,[b] NMR	50	*45*
	1.5 nM	1:2	fluorescence[c]	15	*41*
	23 ± 2 nM	1:1	fluorescence[c]	208	*42*
SL3	∼200 nM	1:1	filter binding[b]	50	*20*
	∼100 nM	1:1	gel shift,[d] NMR, gel filtration	50	*44*
	nd[e]	1:1	ESI-MS	10	*67*
	170 ± 65 nM	1:1	ITC[b]	50	*45*
	∼100 nM^2, ∼1×10^{-19} M^3	2:1, 8:4	gel shift[b]	25	*38*
	∼0.01 nM^2, ∼1×10^{-16} M^3	2:1, 8:4	gel shift[d]	25	*38*
	nd[e]	1:1, 1:2	gel shift[b]	50	*46*
	0.77 nM	1:2	fluorescence[c]	15	*41*
	28 ± 3 nM	1:1	fluorescence[c]	208	*42*
SL4	∼200 nM	1:1	filter binding[b]	50	*20*
	47 ± 14 μM	1:1	gel shift[b]	50	*46*
	11 nM	1:2	fluorescence[c]	15	*41*
	320 ± 30 nM	1:1	fluorescence[c]	208	*42*

[a] Concentration of monovalent cations. [b] Titration of SL with NC as the titrant. [c] Titration of NC with SL as the titrant. [d] Dilution of the SL·NC complex. [e] K_d value not determined.

of the binding stoichiometry and ligand composition, without the possibly disruptive effects of separation techniques on binding equilibria. These unique features have been utilized in this work to determine the stoichiometry and binding affinity of NC for individual hairpins. Competitive binding experiments performed in the simultaneous presence of SL2−SL4 constructs, or structural variants, have helped to establish an unequivocal scale of binding affinity for the three hairpins. The results of this study and the possible implications for understanding the processes of genome recognition and viral assembly are discussed in the context of the current knowledge of the binding activity of NC.

MATERIALS AND METHODS

RNA Preparation. RNA sequences correspond to those present in the Ψ-RNA of the NL4-3 strain of HIV-1 (i.e., SL2, GGCGACUGGUGAGUACGCC; SL3, GGACUAGCGGAGGCUAGUCC; and SL4, GGAGGUGCGAGAGCGUCUCC). RNA constructs were purchased from Dharmacon, Inc. (Lafayette, CO), deprotected according to the manufacturer's recommendations, and extensively desalted by ultrafiltration on Centricon YM-3 devices (Millipore, Bedford, MA). Alternatively, RNA samples were prepared by *in vitro* transcription of synthetic DNA templates using the phage T7 polymerase reaction (*73*). Transcribed RNAs were purified by denaturing gel electrophoresis performed on 20% polyacrylamide gels, and the products of interest were recovered by electroelution from manually excised bands. For the competitive binding experiments, a shorter version of SL3 RNA lacking one nucleotide from each end (SL3-2) was prepared to eliminate any possible signal overlap with SL4. A DNA analogue of SL3 and one containing a tetraloop devoid of nucleobases [i.e., the loop bases $G^9G^{10}A^{11}G^{12}$ were replaced with abasic nucleotides (*41*)] were purchased from the W. M. Keck Biopolymer Laboratory (New Haven, CT) and were called $SL3_{DNA}$ and $SL3_{abasic}$, respectively. The purity of each RNA and DNA sample was confirmed by ESI-FTMS prior to use, while their concentration was determined by UV absorbance, using the following values of molar absorptivity: 190.07 mM^{-1} for SL2, 204.64 mM^{-1} for SL3, 186.55 mM^{-1} for SL3-2, 201.99 mM^{-1} for SL4, 200.44 mM^{-1} for $SL3_{DNA}$, and 136.39 mM^{-1} for $SL3_{abasic}$. Immediately prior to use, each construct was heated to 95 °C for 3 min and then quickly cooled on ice to achieve the proper folding of the hairpin structures.

NC Preparation. An expression vector containing the gene for NC (a gift from M. F. Summers, Howard Hughes Medical Institute, University of Maryland, Baltimore County) was transformed and expressed in *Escherichia coli* BL21(DE3)-pLysE cells. NC was purified under nondenaturing conditions (*44*) and then desalted by ultrafiltration, as described for the RNA samples. The purity and integrity of the protein, including the presence of two coordinated Zn^{2+} ions, were confirmed by ESI-FTMS, while the sample concentration was obtained from the UV absorbance ($\epsilon = 6.41$ mM^{-1}).

Protein−RNA Binding Experiments. Preliminary experiments were carried out by mixing appropriate volumes of stock solutions of NC and individual hairpins in 10 mM ammonium acetate (pH 7.5) to form equimolar mixtures of RNA and protein (10 μM each). These samples were incubated at room temperature for 15 min to ensure that a binding equilibrium was established in solution before ESI analysis. Control experiments were performed using apo-NC samples, which were prepared *in situ* by adding glacial acetic acid to reach a pH of ∼3.0, or by performing ultrafiltration of the holoprotein upon treatment with 20 mM EDTA.

The determination of dissociation constants (K_d) was conducted in 150 mM ammonium acetate (pH 7.5) to weaken the RNA−protein interactions to the point where sufficient unbound RNA could be reproducibly observed within the typical range of working concentrations for the noncovalent complexes (0.1−20 μM). The individual titration of SL4 was carried out by adding increasing amounts of NC to an initial 11.1 μM solution of RNA, while the competitive binding experiments were conducted on solutions containing equimolar concentrations of SL2, SL3-2, and SL4 (5.0 μM each). All experiments were performed in triplicate, and the precision reported for the dissociation constants reflects the overall uncertainty of each K_d determination. The competitive binding experiment including SL3-2, $SL3_{DNA}$, and $SL3_{abasic}$ was performed in a similar fashion by adding NC to equimolar mixtures containing each construct at 10 μM. In this case, a 10 mM ammonium acetate solution was employed to allow for the semiquantitative study of the much weaker complexes provided by the DNA hairpins.

Mass Spectrometry. Immediately prior to analysis, analyte solutions were mixed with 10% 2-propanol to reduce the surface tension and facilitate the achievement of stable spray conditions (*54*). Control experiments performed in the absence of organic modifiers (i.e., 100% aqueous conditions) produced the expected decrease in spray stability, but showed no detectable differences in the state of association of the noncovalent complexes. Consequently, the conditions ensuring the most stable mode of operation were selected in the interest of signal reproducibility. Analyte solutions were introduced into the electrospray source by a syringe pump at a flow rate of 2 μL/min.

Direct infusion analyses were performed on a Bruker Daltonics (Billerica, MA) Apex III FTMS system equipped with a 7 T actively shielded superconducting magnet and an Apollo thermally assisted electrospray source, which includes a metal tubing interface built in house. Source conditions were optimized to allow for the observation of intact noncovalent complexes and included an interface temperature of 120 °C and a difference in potential between the metal tubing and the first skimmer (ΔV_{TS}) of ∼200 V. Control experiments were performed by increasing the temperature to a maximum of ∼160 °C and the ΔV_{TS} to ∼300 V (see Results and Discussion). Spectra were acquired in the negative ion mode and processed using XMASS 6.0.1 (Bruker Daltonics). A resolving power of ∼150000 was typically obtained in broadband mode, and an accuracy of ∼10 ppm or better was achieved by using a three-point external calibration.

Data Analysis. The interpretation of electrospray data containing series of multiply charged ions is facilitated by the high resolving power provided by FTMS. In fact, fully resolved isotopic distributions enable a direct and unambiguous assignment of the charge state of electrosprayed ions by calculating the reciprocal of the mass-to-charge spacing ($\Delta m/z$) between successive isotopic peaks (Figure 2, inset) (*50*). In this way, the possible presence of stoichiometric

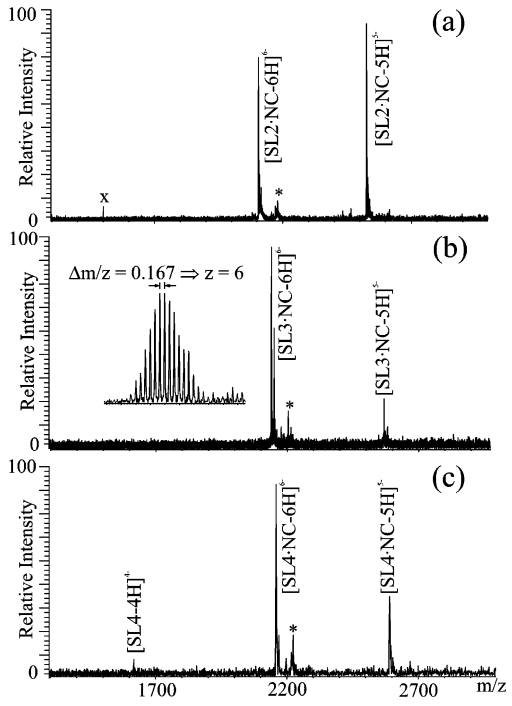

FIGURE 2: ESI-FTMS mass spectra of 10 μM (a) SL2·NC, (b) SL3·NC, and (c) SL4·NC complexes in 10 mM ammonium acetate. The inset shows an expanded view of the −6 charge state of the SL3·NC complex. Asterisks denote an impurity present in the NC sample; the x denotes a Fourier transform alias.

multiples (e.g., 2:2, 3:3, etc.), which could be observed with similar *m*/*z* values at low resolution, can be effectively ruled out at the resolution achieved by these FTMS measurements.

The determination of free versus bound RNA necessary to calculate the K_d values of the complexes was obtained from the initial ligand concentrations by using the molar fractions of the different species in solution (*74*), which were directly assessed from the intensity of the respective peaks (*75*) divided by the charge state. This method relies on the reasonable assumption that there is no significant detection discrimination between free RNA and the corresponding complex in the same sample, which is supported by the observation that any effect on charging produced by protein binding (e.g., charge neutralization by formation of salt bridges, modification of pK_a values of chargeable groups by near-neighbor effects, etc.) can lead to only a partial shift of the charge state distribution, rather than to a complete neutralization of all the charges carried by any given multiply charged ion. The fact that all species involved presented at least three negative charges rules out the possibility of complete neutralization and consequent signal suppression. Taking into consideration all the charge states observed for each species offsets the effects of a shift of charge state distribution, which manifests itself as compensatory changes in the relative signal intensities of successive charge states (e.g., neutralization of one charge will decrease the abundance of −4, but increase that of −3, and *vice versa*). Normalizing the signal intensity by the respective charge state constitutes a simple (albeit imperfect) way to reduce the possible bias due to the fact that different charge states induce different image currents during ion detection in FTMS (*50*).

Rather than plotting the experimental data and finding K_d through a graphical curve fitting procedure, we followed an alternative method to minimize the mathematical steps performed directly on the experimental numerical figures. According to the ESI-FTMS results obtained within the range of concentrations of the titration, the equilibrium under consideration is SL4 + NC ⇆ SL4·NC, for which $K_d = ([SL4][NC])/[SL4·NC]$. At equilibrium, $[SL4] = ([SL4]_0 - x)$ and $[NC] = ([NC]_0 - x)$, where $[SL4]_0$ and $[NC]_0$ are the initial concentrations of RNA and protein before binding, respectively, and x is the bound portion equivalent to [SL4·NC] at equilibrium. Substituting $K_d = ([SL4]_0 - x)(([NC]_0 - x)/x$, the $x^2 - (K_d + [SL4]_0 + [NC]_0)x + [SL4]_0 + [NC]_0 = 0$ quadratic equation can be obtained.

The solution of the quadratic equation provides the concentration of bound SL4, which can be divided by $[SL4]_0$ to express the fraction of bound SL4 at equilibrium. The ratio $x/[SL4]_0$ can be finally compared with the corresponding experimental fraction obtained by ESI-FTMS. The equation solver included in the Graphical Analysis software package (Vernier Software, Beaverton, OR) was employed to find the value of K_d, which minimizes the difference between the experimental fraction of bound SL4 and the corresponding $x/[SL4]_0$ ratio calculated by substituting in the quadratic solution the known initial values of $[SL4]_0$ (constant) and $[NC]_0$ (increasing throughout the titration). This simple method avoids making any assumption concerning binding and reduces the error propagation due to mathematical processing. In fact, the experimental fraction, which carries the largest error, is only used once at the end of each reiteration, when it is compared with the calculated fraction. A curve was calculated back from the reported K_d to provide a graphical visualization of the binding characteristics of the system.

The other dissociation constants were obtained from the competitive binding experiment, including SL2, SL3-2, and SL4, by comparing the ratios of bound to free RNA between SL2 and SL4 and then between SL3-2 and SL4. Because the K_d for SL4·NC under these conditions was provided by the individual titration, the absolute K_d values for SL2 and SL3-2 complexes were readily calculated.

RESULTS AND DISCUSSION

The formation of noncovalent complexes between nucleocapsid protein p7 and RNA hairpins SL2−SL4 of the HIV-1 packaging signal was readily observed by direct infusion ESI-FTMS of neutral solutions prepared by mixing equimolar amounts of protein and RNA samples (Figure 2). The resolution achieved in these measurements (∼150000) enabled us to fully resolve the isotopic distributions of all the species that were detected, thus revealing the charge state of individual ions (see inset) and making the data interpretation unambiguous. The observed molecular masses were found to be in very close agreement with theoretical masses calculated for 1:1 complexes of RNA and protein, based on the respective sequences and including two zinc ions per holo-NC molecule (Table 2) (*67*, *76*, *77*).

Significance of the Noncovalent Complexes Detected by ESI Analysis. A primary concern in studying noncovalent interactions by ESI is to ensure that the experimental results represent as closely as possible the actual solution composition prior to transfer of the analytes to the gas phase. The formation of nonspecific aggregates and the possible dis-

Table 2: Masses for RNA Hairpins and Complexes with NC

	expected mass (Da)	observed mass (Da)
NC	6488.91	6488.87
SL2	6128.86	6128.87
SL3	6457.92	6458.02
SL3-2	5807.83	5807.79
SL4	6473.91	6473.93
SL2·NC	12617.77	12617.87
SL3·NC	12946.82	12946.95
SL3-2·NC	12296.73	12296.69
SL4·NC	12962.82	12963.00

sociation of weakly bound complexes are the two extreme situations that must be carefully considered when evaluating the validity of experimental data concerning noncovalent complexes (*54*, *72*, *78*).

Nonspecific aggregation may occur during the electrospray process in conjunction with high analyte concentrations and is generally characterized by the detection of complexes with compositions and stoichiometries that do not match those expected for the biological system under investigation (*54*, *79*, *80*). The significance of the 1:1 complexes of NC and hairpins was tested by mixing the RNA samples with apo-NC produced by slight acidification (pH ~3.0), or by treatment with metal chelating agents, which are known to induce the loss of Zn^{2+} coordination by the two zinc-finger domains with consequent defolding of the native three-dimensional (3D) structure (*81*−*83*). In both cases, only extremely weak signals were observed for RNA bound to denatured apo-NC data not shown, as compared to those obtained for native holo-NC under otherwise similar analytical conditions, which is consistent with a residual binding activity of randomly structured apo-NC through electrostatic interactions between its numerous positively charged residues and the polyanionic backbone of the nucleic acid counterpart (*15*, *84*, *85*). For this reason, it is reasonable to conclude that the observed 1:1 complexes of RNA and native protein are the product of specific binding interactions in solution and cannot be attributed to artifactual aggregation induced by the selected experimental conditions.

The incidence of dissociation during the transfer of noncovalent complexes to the gas phase can be assessed by employing progressively harsher desolvation conditions, which can be achieved by either increasing the skimmer voltage (or equivalent) in the high-pressure region of the ion source (*60*, *86*−*89*) or increasing the temperature of the capillary interface or drying gas (*54*, *55*, *58*, *60*, *62*, *90*). In our case, substantial increases in the skimmer voltage (or ΔV_{TS}; see Materials and Methods) and interface temperature did not produce any visible effects on the stability of the complexes. Partial gas phase fragmentation of the nucleic acid moiety was induced by voltages nearing the hardware limit; however, no dissociation of the protein−RNA interaction was detected. A similar effect was reported for a DNA−protein complex, which underwent only partial dissociation at the substantially high voltages that resulted in the cleavage of covalent bonds (*60*). While it is very likely that normal desolvation conditions may induce conformational changes in the complexes that could adversely affect the strength of the interactions during the ESI process, the experimental results obtained for the NC−hairpin systems clearly indicate that such changes are not sufficiently drastic to force dissociation during transfer to the gas phase. The solution equilibrium is clearly the only process determining the partitioning between free and unbound species recorded by ESI under the selected conditions. For this reason, it is possible to conclude with a high confidence level that the experimental data provide a truthful representation of the solution composition and binding status of the different components, which is fundamentally important for the determination of solution binding constants by titration methods (*72*).

Modes of Binding of NC with the RNA Hairpins. The possibility of multiple binding modes was tested by adding increasing amounts of NC to constant initial amounts of individual stem−loop hairpins. The observation that only a relatively small fraction of free SL4 was left in the equimolar mixture at 10 mM ammonium acetate (Figure 2c), while no free RNA remained in the spectra of either the SL2·NC or SL3·NC complex (Figure 2a,b), suggested that titration experiments performed under these conditions would not offer an accurate representation of the position of the binding equilibria in solution. Consequently, the salt content was increased to 150 mM to weaken the interactions between protein and nucleic acids (*40*, *62*, *91*, *92*), which resulted in a more gradual increase in the percentage of bound complexes during the titration with no significant impact on the analytical process.

Selected points in the titration of an 11.1 μM solution of SL4 in 150 mM ammonium acetate (pH 7.5) are shown in Figure 3. Subequimolar addition of protein to RNA allowed for the detection of a 1:1 complex and a certain amount of unbound SL4 (Figure 3a). No evidence was found for higher-order complexes involving multiple binding of RNA (e.g., 2:1, 3:1, etc., RNA to protein), despite the excess of SL4 left in solution. Equimolar addition of protein was shown to significantly increase the abundance of the SL4·NC complex and, conversely, decrease the amount of free RNA (Figure 3b). No unbound SL4 was reproducibly observed upon addition of a 2-fold amount of NC (Figure 3c). The SL4·NC complex was still the dominant species, but formation of a small percentage of the SL4·2NC complex was also detected under these conditions. It is interesting to note that a relatively large excess of NC was necessary to induce the binding of a second unit, indicating a large difference in affinity between the first and second equivalent. The fact that all the initial SL4 in solution was completely saturated with one unit before binding of the second became detectable does not support the hypothesis that binding of multiple units may present a cooperative character.

A 10-fold addition of protein afforded the exclusive observation of a SL4·3NC complex, with no evidence for higher-order stoichiometry (Figure 3d). As an effect of higher concentrations, free NC was also detected in the negative ion mode despite its relatively basic character (pI 9.9) (*93*, *94*). Further additions (up to 20-fold protein) produced an expected increase in the magnitude of the signal of free NC, but did not induce the formation of higher-order complexes beyond the described SL4·3NC complex (data not shown). The apparent maximum number of three NC equivalents per SL4 molecule is consistent with the size of this 20mer RNA construct and with the fact that NC is capable of occupying an average of seven (6.8 ± 0.3) nucleotides upon binding to

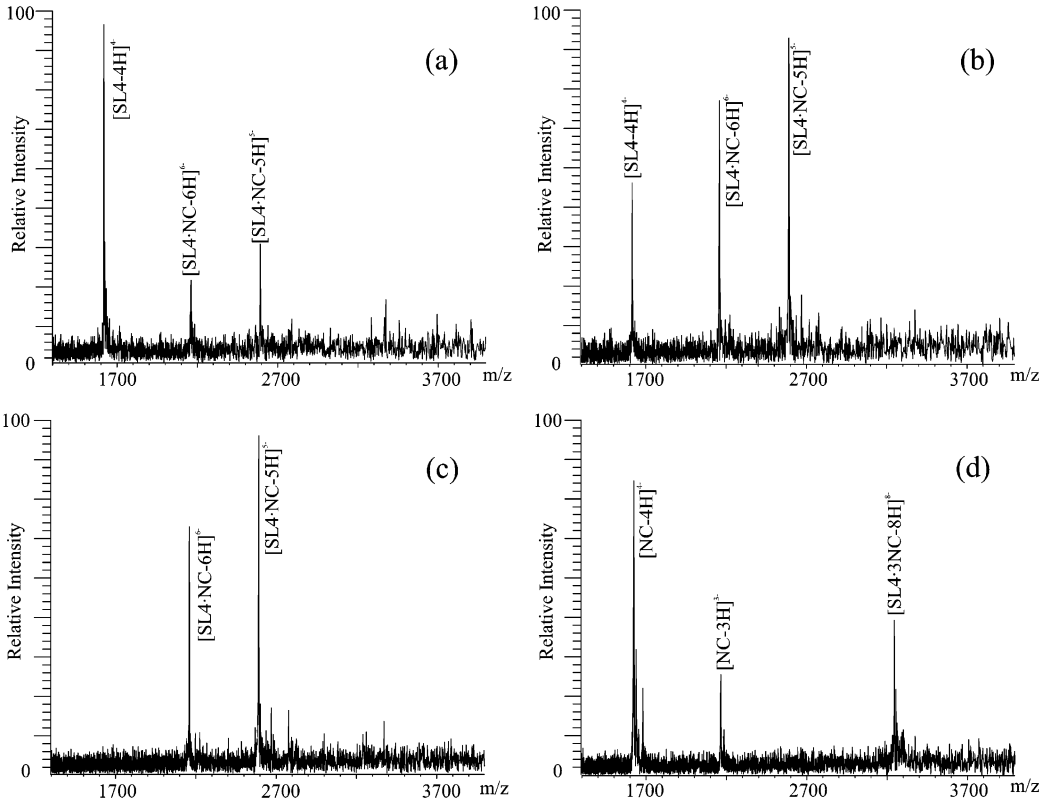

FIGURE 3: ESI-FTMS analysis of the different solutions obtained by adding (a) 0.5× NC, (b) 1× NC, (c) 2× NC, and (d) 10× NC to an initial 11.1 μM solution of SL4 in 150 mM ammonium acetate.

single-stranded DNA, in contrast to ~8 bp for double-stranded DNA (*17*, *95*−*98*). These results corroborate the observation of higher-order binding by gel shift electrophoresis (*46*) and fluorescence quenching (*41*) obtained with different sample concentrations and ionic strength. The fact that species with a stoichiometry exceeding the limit corresponding to the size of the occluded site were not detected by ESI-FTMS offers further confirmation of the absence of nonspecific aggregation during the analytical process.

Analogous qualitative trends were provided by the titration of 19mer SL2 and 20mer SL3 performed under similar experimental conditions [5.0 μM solution of RNA in 150 mM ammonium acetate (pH 7.5)]. In fact, ions corresponding to 1:1 complexes were detected in the presence of sub-equimolar and equimolar amounts of NC. Higher-order binding was observed only upon addition of excess protein, with a maximum binding stoichiometry of 3 equiv of protein per mole of RNA (data not shown), which is also consistent with the size of the constructs and the average size of the site occupied by NC bound to single-stranded DNA. This binding pattern could be explained by a process of defolding of the hairpin structure induced by the initial interaction with the primary, high-affinity, site comprising the loop region and part of the helical stem (*44*, *45*). This interaction could lead to the destabilization of the double-stranded stem (*17*), enabling the lower-affinity binding of NC to the perhaps partially exposed strands of RNA, with a final stoichiometry corresponding to that predicted for unstructured single-stranded DNA.

Affinity of NC for the RNA Hairpins: Competitive Binding. The binding affinity of NC for SL4 was determined from the relative amounts of free and bound RNA observed after progressive addition of the protein to an initial 11.1 μM solution of SL4 in 150 mM ammonium acetate. The titration was limited to the first equivalent of NC. The dissociation constant was calculated by using the procedure described in Materials and Methods, which provided a K_d of 1.3 ± 0.5 μM. Figure 4 provides a graphical representation of the binding curve calculated from the reported value of K_d. A direct correlation of this value with dissociation constants reported in the literature is difficult, as expected from the little consistency of ionic strength, sample concentrations, and experimental design used by the different methods (e.g., dilution vs titration, RNA vs NC as a titrant, etc.). Nevertheless, the figure provided by ESI-FTMS appears to fall within the range delimited by the results of gel shift electrophoresis

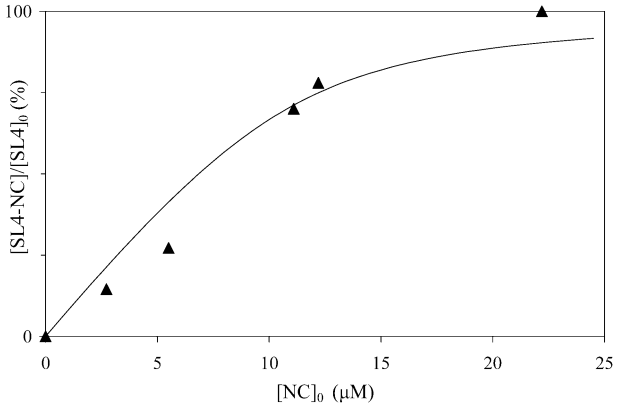

FIGURE 4: Binding curve provided by the titration of 11.1 μM SL4 with NC to form the SL4·NC complex. The curve was obtained for a K_d of 1.3 ± 0.5 μM, which was calculated according to the procedure described in Materials and Methods. The reported precision reflects the overall uncertainty of the K_d determination.

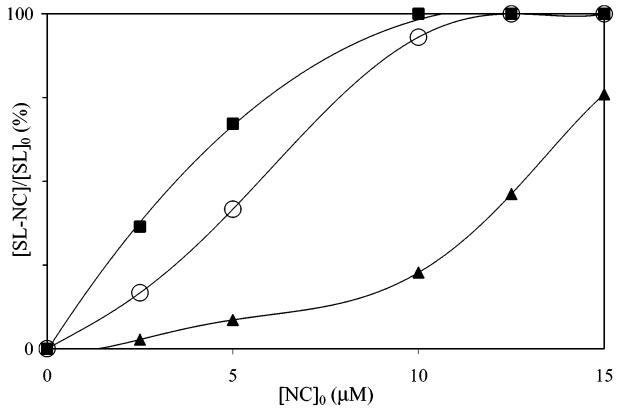

FIGURE 5: Binding curves obtained from competition experiments between SL2, SL3-2, and SL4 (5.0 μM each) in 150 mM ammonium acetate with increasing amounts of NC: (■) SL2·NC, (○) SL3·NC, and (▲) SL4·NC. The procedure employed to calculate the different K_d values is described in Materials and Methods.

and fluorescence quenching (Table 1 and references therein) and leaves no doubts about the identity and integrity of the species included in the calculations.

A competitive binding experiment, which included all three RNA constructs simultaneously, was carried out to determine the dissociation constants of SL2 and SL3-2 (a shorter version of SL3; see Materials and Methods) based on the value obtained separately for SL4. According to this procedure, increasing amounts of NC were added to an equimolar mixture of the three hairpins (5.0 μM each). ESI-FTMS analysis of the competition mixtures found exclusively 1:1 complexes and unbound excess RNA upon subequimolar additions of NC (data not shown). Dissociation constants of 62 $\pm$ 22 and 178 $\pm$ 64 nM were calculated for SL2 and SL3-2, respectively, by using the value of K_d found earlier for SL4 (see Materials and Methods). The competitive binding curves are shown in Figure 5. These values follow the same order of binding affinity obtained by the majority of the methods summarized in Table 1 (i.e., SL2 > SL3 $\gg$ SL4), providing further confirmation of the viability of the ESI-based method.

The presence of an electrostatic component in the interaction between NC and RNA is likely to play a role in the successful observation of the complexes by ESI, but cannot explain by itself the subtle variations of binding affinity to which the method has proven to be sensitive. In fact, the constructs used in our experiments share a similar number of nucleotides (19 for SL2, 18 for SL3-2, and 20 for SL4), and the overall Coulombic attraction between the negatively charged nucleic acids and the positively charged protein is very likely to provide similar contributions to the overall binding strength. Furthermore, the salt content utilized in these experiments (150 mM ammonium) is considered to be sufficient to reduce the contributions of electrostatic interactions to the point where hydrogen bonds and hydrophobic interactions become more important in the balance (*40*, *99*).

The variations in binding affinity within the series are clearly the product of distinct nonelectrostatic interactions that are a function of the different sequences and 3D structures of the constructs employed in the experiments. Systematic studies using short single-stranded oligonucleotides (*40*, *99*) and full-length SL3 variants (*43*) in solutions of intermediate salt content (100−200 mM NaCl) have proven that NC has a strong preference for binding loops with a GGNG sequence, which is matched by GGUG and GGAG in the single-stranded loop of SL2 and SL3, respectively (Figure 1). However, the fact that an SL3 analogue including the SL2 loop GGUG was found to bind more tightly than the native SL3 with the GGAG loop (*43*) does not completely explain the difference in affinity, which should account also for the interactions with the double-stranded stems. The contribution of stem interactions to the overall stabilization is expected to be greater in the SL2·NC complex, where the N-terminal zinc finger (F1) makes specific contacts with the AUA triple-base platform located in the stem region (*45*, *100*), than it is in the SL3·NC complex, where F1 interacts with only the major groove of the helical stem (*44*). On the other hand, the affinity observed for SL4 appears to be somewhat higher than expected from the data offered by an SL3 analogue with SL4's GAGA loop (*101*), suggesting an even greater contribution from stem interactions than for the other two hairpins. In the absence of a high-resolution structure for the SL4·NC complex, the existence of interactions involving the stem's tandem G·U wobbles was revealed by chemical probes, which induced the alkylation of wobble guanines in free SL4, but not in the SL4·NC complex (*102*). In the context of the structure of the complete Ψ-site, a weaker interaction between NC and the GAGA loop would be consistent with the preferential participation of this GNRA-type tetraloop in long-range tertiary contacts with other regions of RNA (*103*, *104*), which may be involved in determining the global folding of the Ψ-site. On the other hand, a stronger interaction of NC with the G·U pairs could have important functional implications related to the general role played by this motif in RNA−protein recognition (*105*−*107*).

The possible contribution of stem interactions to the overall stabilization balance and the importance of the stem 3D structure in modulating the binding strength can be recognized from the results of a competition experiment comparing SL3-2 RNA with an SL3 DNA construct ($SL3_{DNA}$) and a DNA analogue in which the four bases of the tetraloop were replaced with abasic nucleotides ($SL3_{abasic}$). Additions of NC to an equimolar solution of the three constructs in 10 mM ammonium acetate found that the complex with SL3-2 RNA was at least 30 times tighter than that with $SL3_{DNA}$, while the latter was at least 50 times tighter than that with $SL3_{abasic}$ (a representative ESI-FTMS spectrum is provided in Figure 6). The observed SL3-2 > $SL3_{DNA}$ $\gg$ $SL3_{abasic}$ relative scale of binding affinity clearly indicates that NC is involved in stronger interactions with the A-type double-stranded structure typical of RNA than with the B-type helix characteristic of DNA. The fact that NC makes contacts with the major groove of SL3 RNA (*44*) rules out the possibility that hydrogen bonds involving the 2′-hydroxyls of ribose may account for the higher affinity observed for the RNA construct. As expected, eliminating the stabilization contributed by the interactions with the tetraloop bases further weakened the overall binding strength, thus explaining the lowest affinity in the series recorded for $SL3_{abasic}$.

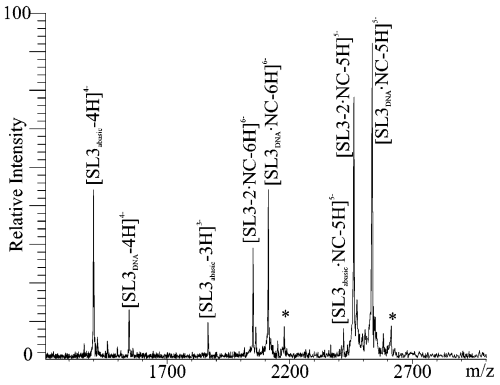

FIGURE 6: Representative ESI-FTMS mass spectrum of the competitive binding of NC to SL3-2 RNA, $SL3_{DNA}$, and $SL3_{abasic}$ in 10 mM ammonium acetate, which shows the situation after addition of 10 μM NC to an equimolar mixture of the nucleic acid constructs (5.0 μM each). Asterisks denote an impurity present in the NC sample.

Conclusions. The application of ESI-FTMS has offered a unique and direct way to investigate *in vitro* the formation of noncovalent complexes between the HIV-1 nucleocapsid protein and RNA hairpins SL2−SL4 of the Ψ-recognition element. Not only has the method been shown to respect the state of association of the species in solution, but it has also been demonstrated to be sensitive to the subtle changes of binding affinity that are linked to the structural context of the binding interactions. The ability to resolve and identify unambiguously the components of simultaneous binding equilibria in solution has enabled us to rule out the formation of complexes with multiple RNA units per equivalent of protein in solutions containing an excess of RNA. The direct observation of a 1:1 stoichiometry as the primary, high-affinity binding mode for the three hairpins offers validation to the spectroscopic and calorimetric techniques, which obtained such a stoichiometry indirectly through data fitting methods. Further binding of NC appears to occur with a significantly lower affinity and without evidence of cooperative effects. The higher-order complexes can only reach a maximum stoichiometry that corresponds to the limit set by the size of the construct and the dimensions of the footprint of NC onto single-stranded nucleic acids, thus implying the defolding of the hairpin's 3D structure.

The absolute values of the dissociation constants of the different hairpins (i.e., 62 ± 22 nM for SL2, 178 ± 64 nM for SL3-2, and 1.3 ± 0.5 μM for SL4) fall within the ranges delimited by established methods. While a fair comparison between K_d values provided by different techniques may be extremely difficult, the competitive binding experiment leaves no doubts about the preference of NC toward the different hairpins, which follows unequivocally the SL2 > SL3 ≫ SL4 series. Operating at intermediate ionic strength highlights the effects of nonelectrostatic interactions, such as H-bonds and hydrophobic interactions, as the main contributors to the affinity difference among hairpins. These variations are due to the contributions provided by the different tetraloop sequences and stem 3D structures. This is clearly exemplified by the higher affinity shown for the A-type RNA double-stranded stem than for the B-type DNA structure of SL3 analogues in competitive binding experiments. The possibility that the tandem G•U wobbles may be more important than the loop region in determining the overall affinity of NC for SL4 deserves to be further investigated and may lead to the elucidation of the role played by this hairpin in the global folding of the complete Ψ-site.

ACKNOWLEDGMENT

We thank Drs. R. L. Karpel and M. F. Summers (University of Maryland, Baltimore County) for many helpful discussions.

REFERENCES

1. Coffin, J. M., Hughes, S. H., and Varmus, H. (1997) in *Retroviruses*, Cold Spring Harbor Laboratory Press, Plainview, NY.
2. Dickson, C., Eisenman, R., Fan, H., Hunter, E., and Reich, N. (1985) in *RNA Tumor Viruses* (Weiss, R., Teich, N., Varmus, H., and Coffin, J., Eds.) pp 513−648, Cold Spring Harbor Laboratory Press, Plainview, NY.
3. Di Marzo Veronese, F., Rahman, R., Copeland, T. D., Oroszlan, S., Gallo, R. C., and Sarngadharan, M. G. (1987) *AIDS Res. Hum. Retroviruses 3*, 253−264.
4. Darlix, J. L., Lapadat-Tapolsky, M., de Roquigny, H., and Roques, B. P. (1995) *J. Mol. Biol. 254*, 523−537.
5. Lever, A. M., Göttlinger, H. T., Haseltine, W. A., and Sodroski, J. G. (1987) *J. Virol. 63*, 4085−4087.
6. Linial, M. L., and Miller, A. D. (1990) *Curr. Top. Microbiol. Immunol. 157*, 25−52.
7. Darlix, J. L., Gabus, C., Nugeyre, M. T., Clavel, F., and Barre-Sinussi, F. (1990) *J. Mol. Biol. 216*, 689−699.
8. Summers, M. F., Henderson, L. E., Chance, M. R., Bess, J. W. J., South, T. L., Blake, P. R., Sagi, I., Perez-Alvarado, G., Sowder, R. C. I., Hare, D. R., and Arthur, L. O. (1992) *Protein Sci. 1*, 563−574.
9. Morellet, N., Jullian, N., De Roquigny, H., Maigret, B., Darlix, J. L., and Roques, B. P. (1992) *EMBO J. 11*, 3059−3065.
10. Berg, J. M. (1986) *Science 232*, 485−487.
11. Weigers, K., Rutter, G., Kottler, H., Tessmer, U., Hohenberg, H., and Kräusslich, H. G. (1998) *J. Virol. 72*, 2846−2854.
12. Lapadat-Tapolsky, M., De Roquigny, H., Van Gent, D., Roques, B. P., Plasterk, R., and Darlix, J. L. (1993) *Nucleic Acids Res. 21*, 831−839.
13. Khan, R., and Giedroc, D. P. (1993) *J. Biol. Chem. 269*, 22538−22546.
14. Berkowitz, R., and Goff, S. (1994) *Virology 202*, 233−246.
15. Lapadat-Tapolsky, M., Pernelle, C., Borie, C., and Darlix, J. L. (1995) *Nucleic Acids Res. 23*, 2434−2341.
16. Tsuchihashi, Z., and Brown, P. O. (1994) *J. Virol. 68*, 5863−5870.
17. Urbaneja, M. A., Wu, M., Casas-Finet, J. R., and Karpel, R. L. (2002) *J. Mol. Biol. 318*, 749−764.
18. Rein, A., Henderson, L. E., and Levin, J. G. (1998) *Trends Biochem. Sci. 23*, 297−301.
19. Darlix, J. L., Cristofari, G., Rau, M., Péchaux, C., Berthoux, L., and Roques, B. (2000) *Adv. Pharmacol. 48*, 345−372.
20. Clever, J., Sassetti, C., and Parslow, T. G. (1995) *J. Virol. 69*, 2101−2109.
21. McBride, M. S., and Panganiban, A. T. (1996) *J. Virol. 70*, 2963−2973.
22. Berkhout, B. (1996) *Prog. Nucleic Acids Res. Mol. Biol. 54*, 1−34.
23. Höglund, S., Öhagen, Å., Goncalves, J., Panganiban, A., and Gabuzda, D. (1997) *Virology 233*, 271−279.
24. Damgaard, C. K., Dyr-Mikkelsen, H., and Kjems, J. (1998) *Nucleic Acids Res. 26*, 3667−3676.
25. Harrison, G. P., and Lever, A. M. L. (1992) *J. Virol. 66*, 4144−4153.
26. Luban, J., and Goff, S. (1994) *J. Virol. 68*, 3784−3793.
27. McBride, M. S., Schwartz, M. D., and Panganiban, A. (1997) *J. Virol. 71*, 4544−4554.
28. McBride, M. S., and Panganiban, A. T. (1997) *J. Virol. 71*, 2050−2058.
29. Clever, J., and Parslow, T. G. (1997) *J. Virol. 71*, 3407−3414.
30. Clever, J. L., Miranda, D., Jr., and Parslow, T. G. (2002) *J. Virol. 76*, 12381−12387.
31. Luban, J., and Goff, S. P. (1991) *J. Virol. 65*, 3203−3212.

32. Schmalzbauer, E., Strack, B., Dannull, J., Guehmann, S., and Moelling, K. (1996) *J. Virol. 70*, 771−777.
33. Surovoy, A., Dannull, J. M. K., and Jung, G. (1993) *J. Mol. Biol. 229*, 94−104.
34. Dannull, J., Surovoy, A., Jung, G., and Moelling, K. (1994) *EMBO J. 13*, 1525−1533.
35. Berglund, J. A., Charpentier, B., and Rosbash, M. (1997) *Nucleic Acids Res. 25*, 1042−1049.
36. Sakaguchi, K., Zambrano, N., Baldwin, E. T., Shapiro, B. A., Erickson, J. W., Omichinski, J. G., Clore, G. M., Gronenborn, A. M., and Appella, E. (1993) *Proc. Natl. Acad. Sci. U.S.A. 90*, 5219−5223.
37. Berkowitz, R. D., Luban, J., and Goff, S. P. (1993) *J. Virol. 67*, 7190−7200.
38. Shubsda, M. F., Kirk, C. A., Goodisman, J., and Dabroviak, J. C. (2000) *Biophys. Chem. 87*, 149−165.
39. Lam, W. C., Maki, A. H., Casa-Finet, J. R., Erickson, J. W., Kane, B. P., Sowder, R. C., II, and Henderson, L. E. (1994) *Biochemistry 33*, 10693−10700.
40. Vuilleumier, C., Bombarda, E., Morellet, N., Gérard, D., Roques, B. P., and Mély, Y. (1999) *Biochemistry 38*, 16816−16825.
41. Maki, A. H., Ozarowski, A., Misra, A., Urbaneja, M. A., and Casas-Finet, J. R. (2001) *Biochemistry 40*, 1403−1412.
42. Shubsda, M. F., Paoletti, A. C., Hudson, B. S., and Borer, P. N. (2002) *Biochemistry 41*, 5276−5282.
43. Paoletti, A. C., Shubsda, M. F., Hudson, B. S., and Borer, P. N. (2002) *Biochemistry 41*, 15423−15428.
44. De Guzman, R. N., Wu, Z. R., Stalling, C. C., Pappalardo, L., Borer, P. N., and Summers, M. F. (1998) *Science 279*, 384−388.
45. Amarasinghe, G. K., DeGuzman, R. N., Turner, R. B., Chancellor, K. J., Wu, Z. R., and Summers, M. F. (2000) *J. Mol. Biol. 301*, 491−511.
46. Amarasinghe, G. K., Zhou, J., Miskimon, M., Chancellor, K. J., McDonald, J. A., Matthews, A. G., Miller, R. R., Rouse, M. D., and Summers, M. F. (2001) *J. Mol. Biol. 314*, 961−970.
47. Aleksandrov, M. L., Gall, L. N., Krasnov, V. N., Nikolaev, V. I., Pavlenko, V. A., and Shukurov, V. A. (1984) *Dokl. Akad. Nauk SSSR 277*, 379−383.
48. Yamashita, M., and Fenn, J. B. (1984) *J. Phys. Chem. 88*, 4671−4675.
49. Comisarow, M. B., and Marshall, A. G. (1974) *Chem. Phys. Lett.*, 282−283.
50. Marshall, A. G., Hendrickson, C. L., and Jackson, G. S. (1998) *Mass Spectrom. Rev.*, 1−35.
51. Ganem, B., Li, Y.-T., and Henion, J. D. (1991) *J. Am. Chem. Soc. 113*, 6294−6296.
52. Baca, M., and Kent, S. B. H. (1992) *J. Am. Chem. Soc. 114*, 3992−3993.
53. Ganguly, A. K., Pramanik, B. N., Tsarbopoulos, A., Covey, T. R., Huang, E., and Fuhrman, S. A. (1992) *J. Am. Chem. Soc. 114*, 6559−6560.
54. Loo, J. A. (1997) *Mass Spectrom. Rev. 16*, 1−23.
55. Beck, J. L., Colgrave, M. L., Ralph, S. F., and Sheil, M. M. (2001) *Mass Spectrom. Rev. 20*, 61−87.
56. Hofstadler, S. A., and Griffey, R. H. (2001) *Chem. Rev. 101*, 377−390.
57. Cheng, X., Harms, A. C., Goudreau, P. N., Terwilliger, T. C., and Smith, R. D. (1996) *Proc. Natl. Acad. Sci. U.S.A. 93*, 7022−7027.
58. Cheng, X., Morin, P. E., Harms, A. C., Bruce, J. E., Ben-David, Y., and Smith, R. D. (1996) *Anal. Biochem. 239*, 35−40.
59. Veenstra, T. D., Benson, L. M., Craig, T. A., Tomlinson, A. J., Kumar, R., and Naylor, S. (1998) *Nat. Biotechnol. 16*, 262−266.
60. Potier, N., Donald, L. J., Chernushevich, I., Ayed, A., Ens, W., Arrowsmith, C. H., Standing, K., and Duckworth, H. W. (1998) *Protein Sci. 7*, 1388−1395.
61. Craig, T. A., Benson, L. M., Tomlinson, A. J., Veenstra, T. D., Naylor, S., and Kumar, R. (1999) *Nat. Biotechnol. 17*, 1214−1218.
62. Kapur, A., Beck, J. L., Brown, S. E., Dixon, N. E., and Sheil, M. M. (2002) *Protein Sci. 11*, 147−157.
63. Deterding, L. J., Kast, J., Przybylski, M., and Tomer, K. B. (2000) *Bioconjugate Chem. 11*, 335−344.
64. Sannes-Lowery, K. A., Hu, P., Mack, D. P., Mei, H. Y., and Loo, J. A. (1997) *Anal. Chem. 69*, 5130−5135.
65. Mei, H. Y., Mack, D., Galan, A. A., Halim, N. S., Heldsinger, A., Loo, J. A., Moreland, D. W., Sannes-Lowery, K. A., Sharmeen, L., Truong, H. N., and Czarnik, A. W. (1997) *Bioorg. Med. Chem. 5*, 1173−1184.
66. Benjamin, D. R., Robinson, C. V., Hendrick, J. P., Hartl, F. U., and Dobson, C. M. (1998) *Proc. Natl. Acad. Sci. U.S.A. 95*, 7391−7395.
67. Loo, J. A., Holler, T. P., Foltin, S. K., McConnell, P., Banotal, C. A., Horne, N. M., Mueller, W. T., Stevenson, T. I., and Mack, D. P. (1998) *Proteins 2* (Suppl.), 28−37.
68. Zhang, S., Van Pelt, C. K., and Wilson, D. B. (2003) *Anal. Chem. 75*, 3010−3018.
69. Greig, M., Gaus, H., Cummins, L. L., Sasmor, H., and Griffey, R. H. (1995) *J. Am. Chem. Soc. 117*, 10765−10766.
70. Griffey, R. H., Hofstadler, S. A., Sannes-Lowery, K. A., Ecker, D. J., and Crooke, S. T. (1999) *Proc. Natl. Acad. Sci. U.S.A. 96*, 10129−10133.
71. Sannes-Lowery, K. A., Griffey, R. H., and Hofstadler, S. A. (2000) *Anal. Biochem. 280*, 264−271.
72. Daniel, J. M., Friess, S. D., Rajagopalan, S., Wendt, S., and Zenobi, R. (2002) *Int. J. Mass Spectrom. Ion Processes 216*, 1−27.
73. Milligan, J. F., and Uhlenbeck, O. C. (1989) *Methods Enzymol. 180*, 51−63.
74. Fabris, D. (2000) *J. Am. Chem. Soc. 122*, 8779−8780.
75. Goodner, K. L., Milgram, K. E., Williams, K. R., Watson, C. H., and Eyler, J. R. (1997) *J. Am. Soc. Mass Spectrom. 9*, 1204−1212.
76. Fabris, D., Zaia, J., Hathout, Y., and Fenselau, C. (1996) *J. Am. Chem. Soc. 118*, 12242−12243.
77. Fabris, D., Hathout, Y., and Fenselau, C. (1999) *Inorg. Chem. 38*, 1322−1325.
78. Fabris, D., and Fenselau, C. (1999) *Anal. Chem. 71*, 384−387.
79. Smith, R. D., and Light-Wahl, K. L. (1993) *Biol. Mass Spectrom. 22*, 493−501.
80. Ding, J., and Anderegg, R. J. (1994) *J. Am. Soc. Mass Spectrom. 6*, 159−164.
81. Hathout, Y., Fabris, D., Han, M. S., Sowder, R. C., Henderson, L. E., and Fenselau, C. (1996) *Drug Metab. Dispos. 24*, 1395−1400.
82. Rice, W. G., Shaeffer, C. A., Harten, B., Villinger, F., South, T. L., Summers, M. F., Henderson, L. E., Bess, J. W., Jr., Arthur, L. O., McDougal, J. S., Orloff, S. L., Mendeleyev, J., and Kun, E. (1993) *Nature 361*, 473−475.
83. South, T. L., and Summers, M. F. (1993) *Protein Sci. 2*, 3−19.
84. McGhee, J. D., and von Hippel, P. H. (1974) *J. Mol. Biol. 86*, 469−489.
85. De Rocquigny, H., Gabus, C., Vincent, A., Fournie-Zaluski, M. C., Roques, B., and Darlix, J. L. (1992) *Proc. Natl. Acad. Sci. U.S.A. 89*, 6472−6476.
86. Schwartz, B. L., Bruce, J. F., Anderson, G. A., Hofstadler, S. A., Rockwood, A. L., Smith, R. D., Chilkoti, A., and Stayton, P. S. (1995) *J. Am. Soc. Mass Spectrom. 6*, 459−465.
87. Meng, C. K., McEwen, C. N., and Larsen, B. S. (1990) *Rapid Commun. Mass Spectrom. 4*, 151−155.
88. Katta, V., Chowdhury, S. K., and Chait, B. (1991) *Anal. Chem. 63*, 174−178.
89. Loo, J. A., Edmonds, C. G., Udseth, H. R., and Smith, R. D. (1990) *Anal. Chim. Acta 241*, 167−173.
90. Robinson, C. V., Chung, E. W., Kragelund, B. B., Knudsen, J., Aplin, R. T., Poulsen, F. M., and Dobson, C. M. (1996) *J. Am. Chem. Soc. 118*, 8646−8653.
91. Record, M. T., Jr., Lohman, T. M., and de Haseth, P. (1976) *J. Mol. Biol. 107*, 145−158.
92. Fisher, R. J., Rein, A., Fivash, M., Urbaneja, M. A., Casa-Finet, J. R., Medaglia, N., and Henderson, L. E. (1998) *J. Virol. 72*, 1902−1909.
93. Kelly, M. A., Vestling, M. M., and Fenselau, C. (1992) *Org. Mass Spectrom. 27*, 1143−1147.
94. Zhou, S., and Cook, K. D. (2000) *J. Am. Soc. Mass Spectrom. 11*, 961−966.
95. Urbaneja, M. A., Kane, B. P., Johnson, D. G., Gorelick, R. J., Henderson, L. E., and Casas-Finet, J. R. (1999) *J. Mol. Biol. 287*, 59−75.
96. Dib-Hajj, F., Khan, R., and Giedroc, D. P. (1993) *Protein Sci. 2*, 231−243.
97. Khan, R., Chang, H.-O., Kaluarachchi, K., and Giedroc, D. P. (1996) *Nucleic Acids Res. 24*, 3568−3575.
98. Mely, Y., de Rocquigny, H., Sorinas-Jimeno, M., Keith, G., Roques, B., Marquet, R., and Gerard, D. (1995) *J. Biol. Chem. 270*, 1650−1656.

99. Fisher, R. J., Rein, A., Fivash, M., Urbaneja, M. A., Casas-Finet, J. R., Medaglia, M., and Henderson, L. E. (1998) *J. Virol. 72*, 1902−1909.
100. Amarasinghe, G. K., De Guzman, R. N., Turner, R. B., and Summers, M. F. (2000) *J. Mol. Biol. 299*, 145−156.
101. Paoletti, A. C., Shubsda, M. F., Hudson, B. S., and Borer, P. N. (2002) *Biochemistry 41*, 15423−15428.
102. Yu, E., and Fabris, D. (2003) *J. Mol. Biol. 330*, 211−223.
103. Jaeger, L., Michel, F., and Westhof, E. (1994) *J. Mol. Biol. 236*, 1271−1276.
104. Abramovitz, D. L., and Pyle, A. M. (1997) *J. Mol. Biol. 266*, 493−506.
105. Cheng, A. C., Chen, W. W., Fuhrmann, C. N., and Frankel, A. D. (2003) *J. Mol. Biol. 327*, 781−796.
106. Mao, H., White, S. A., and Williamson, J. R. (1999) *Nat. Struct. Biol. 8*, 1139−1147.
107. Hainzl, T., Huang, S., and Sauer-Eriksson, E. (2002) *Nature 417*, 767−771.

BI0348922